



# University of HUDDERSFIELD

## University of Huddersfield Repository

Kermani, Majid, Farzaneh, Masoud and Kollar, László E.

The Effects of Wind Induced Conductor Motion on Accreted Atmospheric Ice

### Original Citation

Kermani, Majid, Farzaneh, Masoud and Kollar, László E. (2013) The Effects of Wind Induced Conductor Motion on Accreted Atmospheric Ice. *IEEE Transactions on Power Delivery*, 28 (2). pp. 540-548. ISSN 0885-8977

This version is available at <http://eprints.hud.ac.uk/id/eprint/17723/>

The University Repository is a digital collection of the research output of the University, available on Open Access. Copyright and Moral Rights for the items on this site are retained by the individual author and/or other copyright owners. Users may access full items free of charge; copies of full text items generally can be reproduced, displayed or performed and given to third parties in any format or medium for personal research or study, educational or not-for-profit purposes without prior permission or charge, provided:

- The authors, title and full bibliographic details is credited in any copy;
- A hyperlink and/or URL is included for the original metadata page; and
- The content is not changed in any way.

For more information, including our policy and submission procedure, please contact the Repository Team at: [E.mailbox@hud.ac.uk](mailto:E.mailbox@hud.ac.uk).

<http://eprints.hud.ac.uk/>

# The Effects of Wind Induced Conductor Motion on Accreted Atmospheric Ice

Majid Kermani, Masoud Farzaneh, Fellow, IEEE, and László E. Kollár

**Abstract**-- Galloping of transmission lines creates some cyclic stresses in the conductor and accreted atmospheric ice covering the conductor, which may result in ice failure leading to shedding. Attempts have been made in this research to estimate these cyclic stresses and experimental tests have been conducted to study their effects on atmospheric ice. First, galloping of an ice-covered conductor was simulated by appropriate modification of existing models for bare conductors submitted to galloping. Then, the results of simulation were applied as input for a new model developed using ABAQUS. Results show that the layers of atmospheric ice at the top and bottom of the conductor endure maximum stress. The results of experimental tests with increasing cyclic stress show that ice does not break during galloping at wind velocities below 4.5 m/s. The tests under cyclic loads with constant amplitude reveal that the ice does not fail under stresses corresponding to wind speeds of 3 and 4 m/s, and sometimes fails under stresses arising at a wind speed of 5 m/s.

**Index Terms**—Atmospheric ice, shedding, galloping, cyclic load, Finite element, model, stress.

## I. INTRODUCTION

AFTER many years of improvements in the design of power transmission lines, they are still vulnerable to winds and storms, particularly in cold regions where atmospheric ice accretes on network equipment. The three types of vibrations created by wind on power transmission lines are galloping, Aeolian vibration and wake-induced oscillation. These vibrations are associated with bending and additional tension in the conductors, which can lead to damage to the power network. If ice accumulates on the conductor, then stresses will develop in the ice, which may lead to ice shedding; the physical phenomenon that occurs when the ice coating a conductor suddenly drops off, either naturally or by means of some form of intervention. The dynamic effect of ice shedding on transmission lines has two major categories of concern: electrical and mechanical. Lack of clearance between adjacent conductors, conductors and towers, and conductors and the ground may lead to flashover or electrical shock. From a mechanical point of view, high-amplitude vibrations may cause suspension strings on towers to come into contact, which may break the insulators; whereas the associated excessive tension generated in the conductors may result in large unbalanced loads on towers, possibly leading to tower collapse. As these problems can pose a major threat to the

operational safety of a grid system, the recognition of the nature of stresses in atmospheric ice which cause ice shedding is essential.

Many factors influence ice shedding and most of them emanate from weather changes. One can divide these factors into two categories: the loads which create stresses in atmospheric ice, and the factors which determine the constitutive behaviour of ice. The former category includes wind loads (such as loads from galloping, Aeolian vibration and wake-induced oscillation), ice loads (gravity and ice mass inertia) and other loads such as impact from a flying object and ice shedding in adjacent conductors. The latter category involves the atmospheric conditions during ice accumulation, air temperature during ice shedding, load rate, and ice behaviour in crack nucleation and propagation.

Galloping of suspended conductors has been studied by many researchers [1]-[2]-[3]-[4]. Irvine and Caughey [5] developed a linear theory for free vibration of a uniformly suspended conductor in which both in-plane and out-of-plane motions were considered. The results of this theory have been used by many researchers to model galloping behaviour. Yu et al. [2] developed a three-degree-of-freedom model to describe and predict different galloping behaviours of a single iced electrical transmission line. Ohkuma et al. [4] focused on the effects of wind turbulence on galloping, and tried to explore the galloping behaviour of a four-bundle overhead transmission line in gusty winds. Luongo and Piccardo [3] derived a two-degree-of-freedom model to examine the aeroelastic behaviour of a flexible elastic suspended conductor driven by the mean wind speed blowing perpendicularly to the plane of the conductor. Abdel-Rohman and Spencer [1] used the results of Luongo and Piccardo [3] to study the along-wind and across-wind response motion of a suspended conductor. They also investigated the effect of a vertical viscous damper at a certain location of the conductor.

Only a few of the vast number of publications concerning galloping are mentioned in the above paragraph. To the best of our knowledge, however, none of them discusses in detail the stresses which develop in the ice accretion during the vibration. In this research work, an attempt was made to estimate these stresses and their variations with respect to load variations during galloping. The calculation of conductor galloping motion, developed by Abdel-Rohman and Spencer [1] and Luongo and Piccardo [2], was applied to a conductor covered with atmospheric ice. The results of this calculation are the displacements of each point along the conductor in vertical and transverse directions, as well as the aerodynamic forces and other loads on the ice. These results are used in a new model constructed using the ABAQUS finite element

---

The authors are with Université du Québec à Chicoutimi, Chicoutimi, QC, G7H 2B1 Canada (e-mail: [mkermani@uqac.ca](mailto:mkermani@uqac.ca); [farzaneh@uqac.ca](mailto:farzaneh@uqac.ca); [laszlo\\_kollar@uqac.ca](mailto:laszlo_kollar@uqac.ca))

M. Farzaneh is Chairholder of the NSERC/Hydro-Quebec/UQAC Industrial Chair and Canada Research Chair (CRC) on Atmospheric Icing of Power Network Equipment (CIGELE), M. Kermani and L. E. Kollár are members of this research center.

software. This model provides an estimation of the stress level in different parts of atmospheric ice on the conductor and its variation through a galloping cycle.

Ice failure on transmission lines is examined experimentally by applying gradually increasing and constant amplitude cyclic stresses on ice samples fixed as cantilever beams. The tests with gradually increasing cyclic stress provide a limit stress where ice failure occurs. Experiments with constant amplitude cyclic stresses show whether continuous cyclic loads with amplitudes lower than the limit obtained above cause premature ice failure.

## II. CALCULATION OF GALLOPING LOADS

Galloping of power transmission lines is one of the most important phenomena inducing stresses in the accreted atmospheric ice. The significant deformation of the iced conductor during this high-amplitude vibration induces stresses in the atmospheric ice. This deformation can be estimated by modeling the galloping conductor motion and obtaining the position of each point along the conductor. Therefore, the equation of motion describing conductor galloping will be considered. For a more accurate estimation, the following forces and stresses should be applied on atmospheric ice: aerodynamic forces, additional tension in conductor due to vibration, ice mass inertia and torque due to conductor spring-back.

Owing to the complexity of this problem, we have to simplify some sophisticated aspects of natural conditions, as follows:

- Normally, ice shapes on power transmission lines are not exactly cylindrical and uniform; it is more symmetrical in the middle of the span than in other parts. Nevertheless, it is assumed that ice shape is cylindrical and uniform all along the conductor. However, in the calculation of wind loads on the conductor, the functions of wind force obtained from wind tunnel tests for asymmetrically iced conductors are used.
- Movements and vibrations of towers during galloping are negligible.
- Wind velocity does not change during galloping and it is uniform all along the conductor.

### A. Equation of conductor motion

The basic equations of motion of a suspended conductor are the following [1]-[3]-[5]

$$\frac{\partial}{\partial s}[(T_0 + T_a) \frac{\partial(x + D_x)}{\partial s}] = m \frac{\partial^2 D_x}{\partial t^2} \quad (1)$$

$$\frac{\partial}{\partial s}[(T_0 + T_a) \frac{\partial(y + D_y)}{\partial s}] = -mg + m \frac{\partial^2 D_y}{\partial t^2} + c \frac{\partial D_y}{\partial t} + F_1(s, t) \quad (2)$$

$$\frac{\partial}{\partial s}[(T_0 + T_a) \frac{\partial D_z}{\partial s}] = m \frac{\partial^2 D_z}{\partial t^2} + c \frac{\partial D_z}{\partial t} + F_2(s, t) \quad (3)$$

in which  $s$  is the spatial coordinate along the curved length of the conductor;  $t$  is the time;  $x$  is the coordinate along the conductor span;  $y(s)$  is the conductor static profile;  $D_x(s, t)$ ,  $D_y(s, t)$  and  $D_z(s, t)$  are, respectively, the displacement in the horizontal, vertical and transverse directions (Fig.1),  $m$  is the conductor mass per unit length, including ice mass,  $c$  is the damping coefficient per unit length,  $T_0$  is the static tension;  $T_a$

is the additional dynamic tension in the conductor;  $F_1(s, t)$ , and  $F_2(s, t)$  are, respectively, the external loading per unit length in the vertical and transverse directions.

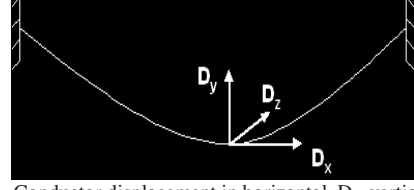


Fig. 1. Conductor displacement in horizontal,  $D_x$ , vertical,  $D_y$ , and transverse,  $D_z$ , directions

When additional dynamic tension is applied to the conductor with accreted ice, this tension is divided between the conductor and the ice according to the following relations:

$$T_{ac} = T_a A_c E_c / (A_c E_c + A_i E_i) \quad (4)$$

$$T_{ai} = T_a A_i E_i / (A_c E_c + A_i E_i) \quad (5)$$

where  $E_i$  and  $E_c$  are Young's modulus of atmospheric ice and conductor, and  $A_i$  and  $A_c$  are cross section areas of the ice and conductor, respectively.

Since the ratio of sag to span in power transmission lines is less than 1:8 and horizontal loads are negligible in our model, we can consider the horizontal displacement  $D_x$  to be equal to zero [1]-[5]. The solution,  $D_y$  and  $D_z$ , of the equations of motion can be obtained by separation of variables:

$$D_y(s, t) = \varphi_1(s)W(t) \quad (6)$$

$$D_z(s, t) = \varphi_2(s)V(t) \quad (7)$$

where  $\varphi_1(s)$  and  $\varphi_2(s)$  are the mode shapes in the transverse and vertical directions respectively, and can be determined as [1]:

$$\varphi_1(s) = A_n \sin(n\pi s / l) \quad n=1, 2, 3, \dots \quad (8)$$

$$\varphi_2(s) = k_0 [1 - \tan(0.5\omega\pi) \sin(\pi\omega s / l) - \cos(\pi\omega s / l)] \quad (9)$$

where  $k_0$  is a constant chosen to make  $\varphi_2(l/2) = 1$ , and  $\omega = \omega_2 / \omega_1$ .  $\omega_1$  and  $\omega_2$ , the natural frequencies in the transverse and vertical directions, can be obtained as follows:

$$\omega_1 = n\pi\sqrt{H/m} / l \quad n=1, 2, 3, \dots \quad (10)$$

$$\omega_2 = q\sqrt{H/m} \quad (11)$$

with  $H$  denoting the horizontal component of conductor tension which can be obtained by solving (12) numerically:

$$d = H[\cosh(mgl / 2H) - 1] / mg \quad (12)$$

where  $d$  is the sag of the conductor. The parameter  $q$  can be calculated from the following equation [5]:

$$\tan(ql / 2) = (ql / 2) - (4 / \lambda^2)(ql / 2)^3 \quad (13)$$

where parameter  $\lambda^2$  takes the form:

$$\lambda^2 = (8d)^2 / (l(HL_e / E_c A_c)) \quad (14)$$

$$L_e = \int_0^l (ds / dx)^3 dx \approx l(1 + 8d^2 / l^2) \quad (15)$$

In order to decrease the number of equations of motion and the complexity of analysis, this problem is solved for first mode shape only ( $n=1$ ). After simplifying (2) and (3), substituting (6) - (15) into them, and applying Galerkin's method, one obtains the equation of motion of the conductor as follows [1]:

$$\dot{W} + 2\xi_1\omega_1\dot{W} + \omega_1^2W + n_5WV^2 + n_6WV^2 + n_7WV^3 = F_1(t) \quad (16)$$

$$\ddot{V} + 2\xi_2\omega_2\dot{V} + \omega_2^2V + n_1V^2 + n_2W^2 + n_3V^3 + n_4VW^2 + F_2(t) = 0 \quad (17)$$

where  $\xi_1$  and  $\xi_2$  are damping ratios in transverse and vertical directions, whereas  $F_1(t)$  and  $F_2(t)$  are determined as below

$$F_1(t) = d_0 + d_1\dot{W} + d_2\dot{W}^2 + d_3\dot{V} + d_4\dot{W}\dot{V} + d_5\dot{V}^2 + \sum_{k=3}^N d_{(2k)}\dot{V}^k + \sum_{k=3}^N d_{(2k+1)}\dot{V}^k\dot{W}^{(k-2)} \quad (18)$$

$$F_2(t) = e_0 + e_1\dot{W} + e_2\dot{W}^2 + e_3\dot{V} + e_4\dot{W}\dot{V} + e_5\dot{V}^2 + \sum_{k=3}^N e_{(2k)}\dot{V}^k + \sum_{k=3}^N e_{(2k+1)}\dot{V}^k\dot{W}^{(k-2)} \quad (19)$$

The coefficients  $n_i$ ,  $d_i$  and  $e_i$  are functions of the diameter of the ice-covered conductor, vibration mode, air density, cable characteristics and mechanical properties of ice [6].

Finally, the equations of motion of a galloping conductor can be written by combining (16) and (17) with (18) and (19), yielding:

$$\dot{W} + 2\xi_1\omega_1\dot{W} + \omega_1^2W + n_5WV^2 + n_6WV^2 + n_7WV^3 = d_0 + d_1\dot{W} + d_2\dot{W}^2 + d_3\dot{V} + d_4\dot{W}\dot{V} + d_5\dot{V}^2 + \sum_{k=3}^N d_{(2k)}\dot{V}^k + \sum_{k=3}^N d_{(2k+1)}\dot{V}^k\dot{W}^{(k-2)} \quad (20)$$

$$\ddot{V} + 2\xi_2\omega_2\dot{V} + \omega_2^2V + n_1V^2 + n_2W^2 + n_3V^3 + n_4VW^2 + e_0 + e_1\dot{W} + e_2\dot{W}^2 + e_3\dot{V} + e_4\dot{W}\dot{V} + e_5\dot{V}^2 + \sum_{k=3}^N e_{(2k)}\dot{V}^k + \sum_{k=3}^N e_{(2k+1)}\dot{V}^k\dot{W}^{(k-2)} = 0 \quad (21)$$

### B. Loads and stresses in atmospheric ice due to conductor bending

The most important type of stress involved in ice shedding from power transmission lines during galloping is the bending stress. When galloping bends the conductor, the atmospheric ice on the conductor resists against this deformation. However, if the force overcomes the resistance of the atmospheric ice, the ice breaks and may shed. The position of each point along the conductor during galloping (results of the calculations presented in Section 2.A) will be used in the ABAQUS model to determine the stresses developing in atmospheric ice.

#### • Aerodynamic forces

As mentioned above, aerodynamic forces cause conductor galloping, and the ensuing movement can produce bending moment and additional tension in the conductor. However, these forces apply some loads directly on the accreted ice too. Equations (18) and (19) express the loads of the aerodynamic force per unit length in the transverse and vertical directions, respectively. To take into account the effect of these forces on a piece of atmospheric ice in the middle of a span, it is sufficient to apply them in the ABAQUS model as a distributed force on the ice (see Fig. 2).

#### • Torsional loads

Power transmission conductors are very flexible and tend to rotate when ice builds up asymmetrically on their surface. Due to such rotation, the ice mass tends to be evenly distributed on the surface of the conductor. This can explain why the ice shape observed on transmission lines is predominantly circular. During ice accretion, when the ice on

the conductor is not symmetric, two factors can apply torsional load on the conductor, ice weight and aerodynamic force due to wind speed. However, when ice accumulates on the conductor and takes a cylindrical shape, the torsional load due to wind becomes negligible. The rotational angle of the iced conductor depends upon the torsional rigidity of the conductor and the amount of ice accreted on it.

The relationship between the rotation of the conductor at mid-span around its centerline,  $\theta$ , and the torque at the suspension points,  $T_A$ , due to conductor spring back can be written as follows:

$$T_A L / 2GJ = \theta \quad (22)$$

where  $GJ$  is torsional rigidity of conductor,  $L$  is conductor length, and constant ice thickness is assumed along the entire span. Once  $\theta$  is known, the spring-back torque,  $T_C$ , which is applied by the conductor to the end point of a piece of ice located in the middle of the span, can be determined as follows:

$$T_C = 2\theta L_1 GJ / L^2 \quad (23)$$

where  $L_1$  is the length of piece of conductor (torque in Fig. 2). Since a short piece of the conductor-ice composition in the middle of the span is analyzed, i.e.  $L_1 \ll L$ , the torque,  $T_C$ , is significantly smaller than the other loads discussed above.

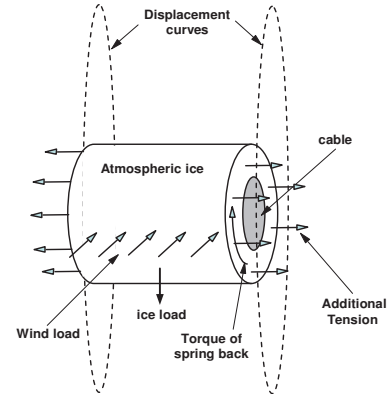


Fig. 2. Loads and movement of a piece of conductor on corresponding curves

#### • Additional tension in the conductor and the ice

As mentioned above, conductor motion during galloping induces additional tension in the conductor and the atmospheric ice. The stresses due to these additional tensions are calculated using the following formulae:

$$\sigma_c = E_c (ds' - ds) / ds \quad (24)$$

$$\sigma_i = E_i (ds' - ds) / ds \quad (25)$$

where  $ds'$  is the deformed conductor segment. These terms were considered in the model developed in ABAQUS (additional tensions in Fig. 2).

#### • Load due to ice mass inertia

The ice load is induced by acceleration due to conductor motion or gravity force. In this model the effect of this load is calculated using the ABAQUS software.

### C. Calculation of forces and displacements

In order to obtain the displacement of each point of conductor during galloping (as mentioned in Section 2.A), the constants  $n_i$ ,  $d_i$ , and  $e_i$  in (20) and (21) should be determined first. These constants together with the initial conductor tension,  $T_0$ , and the natural frequencies in transverse and vertical directions,  $\omega_1$  and  $\omega_2$ , are calculated by a code written in MAPLE. The output data of this code are scalars corresponding to  $T_0$ ,  $\omega_1$  and  $\omega_2$ , as well as three matrices providing the constants  $n_i$  ( $1 \times 7$ ),  $d_i$  ( $1 \times 15$ ) and  $e_i$  ( $1 \times 15$ ).

The conductor motion during galloping is simulated by a program developed in MATLAB. All the results provided by the MAPLE code, the conductor and ice characteristics, the wind velocity,  $U_0$ , and the damping ratios in the vertical and transverse directions,  $\xi_1$  and  $\xi_2$  are defined as input data for the MATLAB implementation. This program solves (20) and (21) numerically and determines the displacement of the two ends of a piece of conductor with ice in the middle of the span. Furthermore, it computes the aerodynamic forces on the ice, the torque applied to the ice due to conductor spring-back, and the additional tension in the conductor and the ice. All of these values are tabulated as time functions, and then are used as loads and displacements in the ABAQUS model described in the next section.

### III. MODELING STRESS VARIATION DURING GALLOPING

The simulation of conductor motion and the load calculation provide all the parameters needed to determine the stress in the ice and its variation during galloping. A model consisting of a part of conductor with uniform cylindrical ice accretion is designed with ABAQUS, which then computes the stress developing in the ice through one or more cycles of galloping. The curves representing conductor motion at each end of the modeled piece, as sketched in Fig. 2, are obtained as output data of the MATLAB program. The additional conductor tension and aerodynamic forces are also added as input data, while the effect of ice load and inertia is calculated by ABAQUS. Fig. 2 shows schematically the movement of a piece of conductor, as well as the forces and the torque applied on the accreted ice.

The analysis was carried out in the Dynamic Explicit condition mode with ABAQUS, which uses a consistent, large-deformation theory and where the model can undergo large rotations and large deformation.

As is the case for all finite element simulations, simulation results are affected by the element type, shape, and location, as well as the overall number of elements used in the mesh. Greater mesh density yields more accurate results. As the mesh density increases, the analysis results converge to a unique solution, and the computer time required for the analysis increases. In the present dynamic explicit simulation however, stability plays a key role and depends on a complex set of interacting factors such as mesh size, material state and time increment. Since the stability limit is roughly proportional to the shortest element dimension, it is advantageous to keep the element size as large as possible [7].

Therefore, the mesh size was chosen as a compromise between these two conditions. Among the element types available in ABAQUS dynamic explicit, the type C3D8R for cable and ice presented the best results, and the stability limit was the determining factor in selecting the size of the elements. The C3D8R is a three-dimensional element with 8 nodes, and it is suitable for continuum stress/displacement analysis with reduced integration. Fig. 3 shows the mesh in the modeled part of the ice and cable.

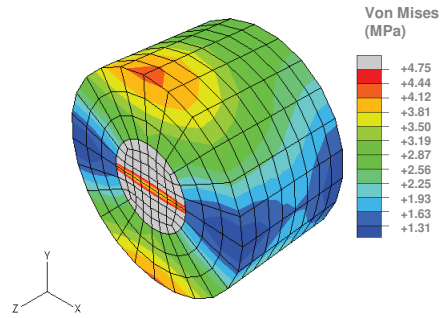


Fig. 3. Illustration of mesh and stress distribution in cable and atmospheric ice for wind speed of 6 m/s.

The variations of transverse and vertical displacements, aerodynamic forces, additional tension in the conductor and the ice were tabulated in 8 tables. Each table has two columns, the first containing the time data, and the other listing the above-mentioned parameters at each instance. The total time of analysis varies between 3.11 s and 3.33 s for wind forces ranging between 3 m/s to 6 m/s, respectively. In order to have more accurate estimation, both ends of the conductor-ice piece at the beginning of the analysis were set in the positions which represent the initial shape of the ice and conductor before any deformation. The ice was assumed to adhere strongly to the conductor surface without sliding and separation.

### IV. RESULTS OF THE MODEL

The preliminary calculations with MAPLE, the galloping simulation with MATLAB and the stress analysis in ABAQUS were applied to a typical example. Table 1 shows the characteristics of the span, conductor and ice considered in this example.

Preliminary calculations were first carried out with the data presented in Table 1, and then the galloping of the conductor-ice composition was simulated. The trajectory of the mid-point of the conductor is shown in Fig. 4, and it is clear that the amplitude of the vertical motion is significantly greater than that of the transverse motion.

The data presented in Table 1 and the results of calculations discussed in Section 3 were applied as input for the stress analysis on a piece of conductor-ice composition in the middle of the span. The length of this piece was set at 10 cm.

The Von Mises and normal stresses in an element located at the external layer of the ice at the bottom of the conductor were calculated during one cycle of galloping and the results for various wind speeds are shown in Figs. 5 and 6. According to Fig. 5, the Von Mises stresses reach their maximum values

at around 1.2 s and 2.8 s, when the mid-point of the conductor is at the highest and lowest position of its trajectory, respectively. Numerically, these maximum values at wind speed of 6 m/s are 7.33 MPa and 4.54 MPa. According to Fig. 4, the vertical displacement of the conductor reaches its limits twice in one cycle: first when the mid-point of the conductor is at the highest position of its trajectory (at 1.2 s), and second when this point reaches the lowest position (at 2.8 s). The stress is greater in the first case, because in this situation, the transverse position of the mid-point of the conductor is the farthest from its location in static equilibrium, while it is the nearest when the mid-point is at the lowest position.

Table 1. Characteristics of the span, conductor and ice

Parameter	Value	Unit
Conductor type	BERSIMIS ACSR	---
Conductor diameter	35.1	Mm
Young's modulus of conductor	62	GPa
Mass per unit length of	2.185	kg/m
Conductor torsional rigidity	351	N.m/Rad
Conductor cross-section area	725.2	mm <sup>2</sup>
Span length	300	M
Conductor sag	8.04	M
Ice type	Hard rime and glaze	---
Ice thickness on conductor	25	Mm
Density of ice	900	Kg/m <sup>3</sup>
Young's modulus of ice	9	GPa
Wind velocity	3, 4, 5, 6	m/s
Rotation angle due to ice accretion at span centre	405°	Degree

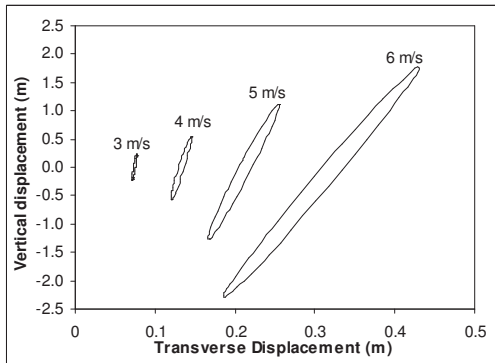


Fig. 4. The trajectory of mid-point of conductor during galloping at various wind speeds.

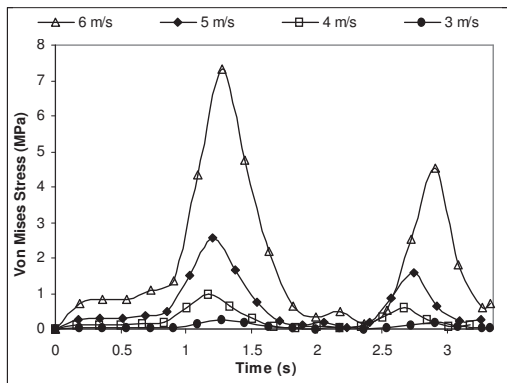


Fig. 5. Cyclic stresses at various wind speeds in the external layer of atmospheric ice.

As shown in Fig. 4, when wind speed increases from 3 to 6 m/s galloping amplitude increases from 0.5 to 2 m while the

galloping frequency reduces from 0.324 to 0.3 Hz, respectively. Considering the significant increase in stress level in atmospheric ice due to the variation of wind speed (Fig. 5), it becomes clear that variation of stresses in atmospheric ice is more directly related to variations in amplitude rather than to changes in galloping frequency.

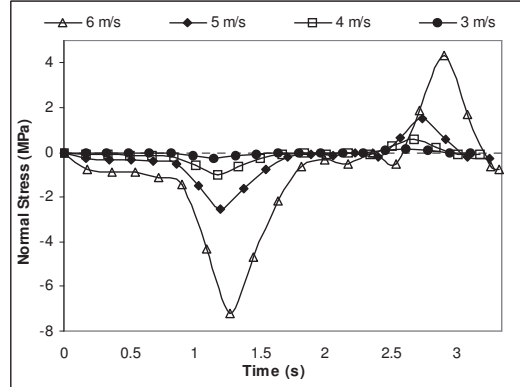


Fig. 6. Normal stresses at various wind speeds in the external layer of accreted ice.

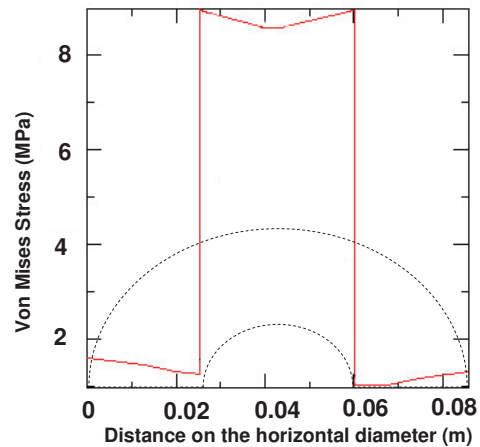


Fig. 7. Stress distribution along horizontal diameter of conductor-ice composition for wind speed of 6 m/s.

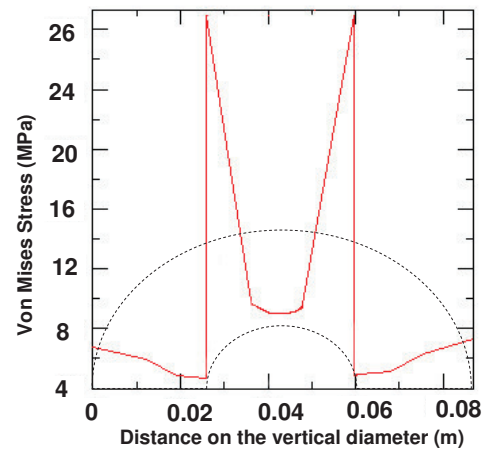


Fig. 8. Stress distribution along vertical diameter of conductor-ice composition for wind speed of 6 m/s.

Fig. 6 shows normal stresses parallel to conductor axis for the same element as in Fig. 5. When the conductor approaches

its highest position, the element will be under compression. The direction of stresses changes when the conductor approaches its lowest position. Obviously, the elements which are on the neutral axis bear the minimum normal stress arising from the additional horizontal tension caused by the conductor motion. Figs. 7 and 8 show the distribution of Von Mises stress along the horizontal and vertical diameters of the iced conductor for a wind speed of 6 m/s in the middle of the 10-cm piece. As expected, stress in the internal layers of the ice (and conductor) is less than that in the external layers.

Readers are referred to Kermani (2007) for more information about stress distribution in atmospheric ice on the conductor during galloping.

## V. EXPERIMENTAL TESTS ON ATMOSPHERIC ICE

In order to investigate ice failure on power transmission lines during galloping, a dynamic load similar to that simulated in the presented model was applied on atmospheric ice with an MTS material test machine. The amplitude and frequency of load were set according to the results of the developed model.

The ice accumulation conditions for this study were created in the CIGELE atmospheric icing research wind tunnel, which is a closed-loop (air-recirculated) low-speed icing wind tunnel. Icing conditions as those encountered during various icing processes in nature can be simulated in this tunnel. For more information about the characteristics of this equipment see [8].

Atmospheric ice was accumulated on an aluminium cylinder (diameter 78 mm and length 590 mm) placed in the middle of the test section of the wind tunnel and rotated at a constant speed of 2 rev/min. Before ice accumulation, the cylinder was cleaned with alcohol and set in place for two hours while the system was cooling down. Once the accumulation was completed, the cylinder was removed from the test section and the accumulated ice was cut with a warm aluminium blade to avoid any mechanical stress that might cause cracks. The resulting ice slices were then carefully prepared using a microtome. The average time interval between ice accumulation and cyclic tests was 5 hours.

Specimen dimensions, as mentioned in ASTM (American Society for Testing and Materials), were determined by averaging three measurements of the three axes of the samples. The guidelines recommended by the IAHR (International Association of Hydraulic Engineering and Research) working group on test methods [9] were used for preparing the specimens.

Air speed that typically leads to natural glaze ice formation ranges from ultra low to medium speeds. In order to make the experimental work more manageable and to obtain a more uniform ice layer, the air velocity value of 10 m/s was chosen. The ambient temperature of -10 °C was selected for the accumulation of atmospheric ice as representative of medium icing conditions. The LWC (liquid water content) for icing conditions in nature varies between 0.5 g/m<sup>3</sup> to 10 g/m<sup>3</sup>, which is within the range achievable in the wind tunnel. In this study the LWC was set at 2.5 g/m<sup>3</sup> in order to obtain solid and uniform atmospheric ice. The mechanical properties of ice can

be influenced by test conditions such as temperature, specimen size, loading rate, failure mode, etc. Considering this, the test conditions were chosen very carefully for this study.

Material tests were carried out at three temperatures -3, -10 and -20 °C, and five specimens were tested for each temperature. The specimens were kept at the test temperature for two hours before each test. The ice specimens were fixed as cantilever beams where the bending force was applied to the end of the beam of atmospheric ice. According to [9], the ratio of beam width to ice crystal size must be  $\geq 10$  in order to eliminate the grain size effect for beams of freshwater ice (which has the closest structure to atmospheric ice). Accordingly, the following dimensions were chosen for our specimens: beam width ( $w$ ) 40 mm, beam thickness ( $h$ ) 20 mm and beam length ( $L$ ) 100 mm.

## VI. TEST RESULTS AND DISCUSSION

The direction of bending force was changed twice during each cycle and its amplitude was gradually increased from zero until the beam failure with an increasing rate of 2 N/cycle. The frequency of this cyclic load was that which occurs during galloping of the conductor at wind velocity of 5 m/s. Fig. 9 shows the configuration of this cyclic test. A typical stress-time graph is shown in Fig. 10.

The individual and average values of bending stress of atmospheric ice at failure are shown in Table 2. The bending stress  $\sigma_f$  was calculated from the elastic beam theory using the equation:

$$\sigma_f = \frac{6FL}{wh^2} \quad (26)$$

where  $F$  is the failure load,  $L$  is the length of the beam,  $w$  and  $h$  are width and height of the beam, respectively, measured at the failure plane.

Tests in which fracture occurred at distances greater than 4 mm from the root of the ice beam (greater than 4 % of the beam length) were excluded from the values listed in Table 2. Only 3 out of 18 tests were discarded for this reason.

The error associated with any particular measurement of bending strength can be determined from the accumulated error associated with all parameters. The uncertainty of  $F$  is 0.25% and that of beam length is 4%. The error for  $w$  and  $h$  corresponds to the one associated with the measurement error of the caliper used to measure the dimensions of the beams and with the scatter in the measurement, which is 0.01mm. Therefore, the total uncertainty in any single measurement of the bending strength is 4.38%. It is worthwhile to notice that the inherent scatter in the test results is considerably greater than this.

The ice failure occurs between 1.75 MPa and 3.46 MPa, as presented in Table 2. According to ABAQUS model results, wind velocities of 4.5 m/s and 5.2 m/s can produce stress levels of 1.75 MPa and 3.46 MPa, respectively, in atmospheric ice on the conductor during galloping. The results of the tests also revealed that the bending strength of atmospheric ice under cyclic loads depends slightly on test temperature. This is not in accordance with previous investigation conducted by Kermani et al.[10] to measure the bending strength of

atmospheric ice fixed as a simple support beam, and its dependence on test temperature and load rate. The temperature effect was not seen in that study at higher load rates when the loading condition is similar to cyclic loads in terms of deformation speed. This means that the probability of ice shedding during galloping in colder temperatures is higher than warm temperatures (below freezing point).



Fig. 9. Configuration of cyclic load test on atmospheric ice .

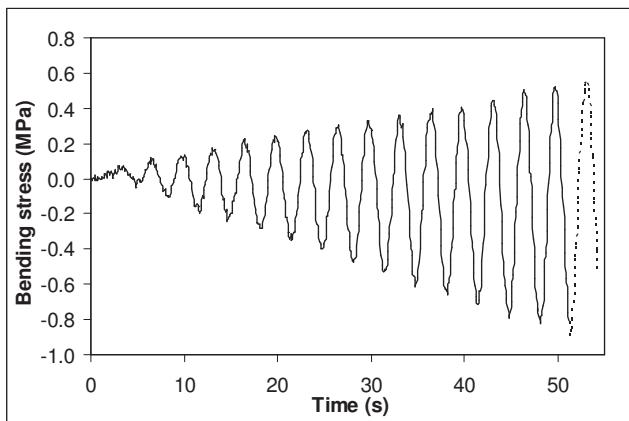


Fig. 10. Cyclic stress in atmospheric ice.

Table 2. Results of cyclic stress on atmospheric ice accumulated at  $-10^{\circ}\text{C}$ .

Test #	Test temperature ( $^{\circ}\text{C}$ )	Stress at failure (Mpa)	Number of Cycles to failure	Ave. of stress at failure (MPa)
1	-3	3.26	53	2.854
2	-3	2.30	39	
3	-3	2.77	49	
4	-3	2.71	50	
5	-3	3.23	67	
6	-10	1.75	31	2.516
7	-10	2.75	52	
8	-10	3.21	62	
9	-10	2.75	61	2.47
10	-10	2.11	47	
11	-20	2.08	49	
12	-20	2.41	50	
13	-20	1.98	43	
14	-20	2.42	57	
15	-20	3.46	51	

Fifteen tests were conducted to study the ice fracture due to continuous cyclic load and fatigue crack propagation.

During these tests, the effects of repetitive low amplitude loads on resistance of ice against crack propagation and fracture were investigated. The results of these tests are given in Table 3. It is observed that low amplitude loads (i.e. less than 2.5 MPa, such as stresses developing in atmospheric ice during Aeolian vibration or galloping due to wind speeds of 4 m/s and less) does not cause premature ice fracture. However, the bending stress of 2.5 MPa is very close to the bending strength of ice [10]; therefore the specimen was broken after a few cycles in two cases.

Table 3. Results of constant amplitude cyclic load on atmospheric ice accumulated at  $-10^{\circ}\text{C}$  and tested at  $-10^{\circ}$ .

Test #	Wind speed (m/s)	Corresponding Bending stress (MPa)	Number of tests	Number of cycles	Result
1	3	0.3	5	2000	Not Failed
2	4	1.0	5	2000	Not Failed
3	5	2.5	3	2000	Not Failed
4	5	2.5	1	31	Failed
5	5	2.5	1	6	Failed

Although the von Mises stress is not equivalent to the bending stress, it mainly arises from the bending load in our case. The Von Mises stress for wind speeds of 3 m/s and 4 m/s is too low to cause ice fracture. For wind speed 5 m/s, however, the stress developing in the atmospheric ice is close to the limit of its bending strength, which means that at wind velocities around 5 m/s and under the conditions assumed in this paper, the ice on the conductor may break and shed due to crack propagation created by cyclic loads. For wind speed 6 m/s, where the von Mises stress is significantly greater than the bending strength of ice, our model predicts ice fracture from the part of the conductor under examination. Ice failure is initiated at the top and bottom sides of the accreted ice sheath, because stresses are higher at these locations, whereas stress level does not exceed the bending strength in the lateral elements at the left and right sides of the conductor.

## VII. CONCLUSION

This paper presents a finite element model for estimating the level of cyclic stresses during galloping of an overhead conductor with accreted atmospheric ice. In order to determine the displacement and load data which serve as input for this model, galloping of an iced conductor was simulated. Equations of conductor motion derived for galloping in former publications were applied to an iced conductor, and solved by a MATLAB code to obtain time histories of conductor motion, aerodynamic forces, additional horizontal tension acting in the conductor during vibration and torque due to spring-back. For this purpose, a 10-cm-long piece of iced conductor at mid-span was considered, with input data being determined at the two end points of the piece. The finite element model was constructed using the ABAQUS commercial software for calculating the stresses in the atmospheric ice accreted on the conductor. The model revealed that the higher stresses occurred along the vertical diameter of the ice when the mid-point of the conductor reached the highest or lowest position of its trajectory. In order to study the behaviour of atmospheric

ice under cyclic stresses, bending tests were conducted on ice beams. The frequency of cyclic stresses was set as the one that applies on atmospheric ice for wind speed 5 m/s. The results of these tests show that atmospheric ice does not fail at cyclic stresses below 1.75 MPa, which corresponds to a wind speed of 4.5 m/s; and ice certainly fails at cyclic stresses above 3.46 MPa or, correspondingly, at wind speeds above 5.2 m/s. The tests with constant amplitude cyclic load also showed that the cyclic stresses due to wind speeds of 3 m/s and 4m/s could not cause premature fracture of atmospheric ice. The cyclic stresses corresponding to wind speed 5 m/s, however, may break the ice, whereas the cyclic stresses created at wind speed 6 m/s will certainly cause ice fracture according to the results of the ABAQUS model. Using the method and model proposed in this investigation, the level of stress in atmospheric ice may be estimated for any other loading condition.

### VIII. ACKNOWLEDGEMENTS

This work was carried out within the framework of the NSERC/Hydro-Quebec/UQAC Industrial Chair on Atmospheric Icing of Power Network Equipment (CIGELE) and the Canada Research Chair on Engineering of Power Network Atmospheric Icing (INGIVRE) at Université du Québec à Chicoutimi. The authors would like to thank the CIGELE partners (Hydro-Québec, Hydro One, Réseau Transport d'Électricité (RTE) and Électricité de France (EDF), Alcan Conductor, K-Line Insulators, Tyco Electronics, CQRDA and FUQAC) whose financial support made this research possible.

### IX. REFERENCES

[1] Abdel-Rohman, M., and Spencer, B. F., 2004, "Control of Wind-Induced Nonlinear Oscillations in Suspended Conductors." *Nonlinear Dynamics*, 37, 341-355.

[2] Yu, P., Desai, Y. M., Shah, A. H., Popplewell, N. , 1993, "Three-degree-of-freedom model for galloping. Part II: Solutions." *Journal of Engineering Mechanics*, 119(12), 2426-2448.

[3] Luongo, A., and Piccardo, G. ,1998, "Non-linear galloping of sagged conductors in 1:2 internal resonance." *Journal of Sound and Vibration*, 214 (5), 915-940.

[4] Ohkuma, T., Kagami J., Nakauchi H., Kikuchi T., Takeda K., Marukawa H., "Numerical Analysis of Overhead Transmission Line Galloping Considering Wind Turbulence." *Electrical Engineering in Japan*, 131(3), 1386-1397, (2000)

[5] Irvine, H. M., and Caughey, T. K., "The linear theory of free vibration of a suspended conductor." *Proc. R. Soc. Lond. A*, 341, 299-315, (1974)

[6] Kermani, M., "Ice shedding from conductors and conductors - a model of cracking activity of atmospheric ice in brittle regime", Ph.D. thesis, University of Quebec at Chicoutimi, QC, Canada, (2007).

[7] ABAQUS theory manual, Version 6.5, ABAQUS Incorporation, (2005)

[8] Kermani, M., Farzaneh, M., Gagnon, R. E., "Compressive strength of atmospheric ice", *Cold Regions science and technology*, Vol. 49, PP 195–205, (2007).

[9] Schwarz, J., Frederking, Gavrilov, R., Petrov, I., Hirayama, K., Mellor, M., Tryde, P. and Vaudrey, K., "Standardized testing methods for measuring mechanical properties of ice", *Cold Regions Science and Technology*, Vol. 4, PP 245-253, (1981).

[10] Kermani, M., Farzaneh, M., Gagnon, R. E. "Bending Strength and Effective Modulus of Atmospheric Ice", *Cold Regions Science and Technology*, Volume 53, Issue 2, PP. 162-169, (2008).

### X. BIOGRAPHIES



**Majid Kermani** received his B.Sc and M.Sc. degrees in Mechanical Engineering from Tehran Polytechnic University of Iran, in 1993 and 1998, respectively. In 2004, he joined CIGELE/INGIVRE at the University of Quebec at Chicoutimi as Ph.D. student and finished his study in 2007. He continues his research in CIGELE/INGIVRE as Postdoctoral Fellow in theoretical and experimental modeling of ice shedding and mechanical properties of atmospheric ice.



**Masoud Farzaneh** (M'83-SM'91-F'07) is Director-founder of the International Research Center CENGIVRE, Chairholder of the CIGELE NSERC/Hydro-Quebec/UQAC Industrial Chair and of the INGIVRE Canada Research Chair related to power transmission engineering in cold climate regions. He authored or co-authored more than 500 technical papers, and 18 books or book chapters. Prof. Farzaneh has so far trained more than 100 postgraduate students and postdoctoral fellows. Actively involved with CIGRÉ and IEEE, he is Convenor of CIGRE WG B2.44 on coatings for protection of overhead lines during winter conditions, and member of the Executive Committee of CIGRE Canada. He is currently Administrative Vice-President of IEEE DEIS, and member of the Editorial Board of IEEE Transactions on Dielectrics and Electrical Insulation. He is Fellow of IEEE, Fellow of The Institution of Engineering and Technology (IET) and Fellow of the Engineering Institute of Canada (EIC). His field of research encompass high voltage and power engineering including the impact of cold climate on overhead transmission lines. His contributions and achievements in research and teaching have been recognized by the attribution of a number of prestigious prizes and awards at national and international levels.



**László E. Kollár** received a M.Sc. degree in Mechanical Engineering from the Budapest University of Technology and Economics, Hungary in 1997, a Ph.D. degree in Mechanical Engineering from the same university in 2001, and a M.Sc. degree in Mathematics from the University of Texas at Dallas, USA in 2002.

In 2002, he joined CIGELE NSERC/Hydro-Quebec/UQAC Industrial Chair and INGIVRE Canada Research Chair at the University of Quebec at Chicoutimi as a Postdoctoral Fellow, and he became a Research Professor on grant in 2005. His research interests include theoretical and experimental modeling of atmospheric icing processes and ice shedding from cables. He previously worked on the modeling of controlled unstable mechanical systems with time delay. He authored or co-authored more than 50 journal and conference papers and a book chapter.